IEEE Access
Multidisciplinary | Rapid Review | Open Access Journal

Received 31 March 2025, accepted 2 June 2025, date of publication 12 June 2025, date of current version 23 June 2025.

Digital Object Identifier 10.1109/ACCESS.2025.3579340

RESEARCH ARTICLE

Fast and Scalable Dynamic Gas Network Modeling and Simulation Framework With Gas Composition Tracking

YIFEI LU[1,2], (Graduate Student Member, IEEE), ANDREW IVAN SULIMRO[1], THIEMO PESCH[1], AND ANDREA BENIGNI[1,2,3], (Senior Member, IEEE)

[1]Institute of Climate and Energy Systems, Energy Systems Engineering (ICE-1), Forschungszentrum Jülich, 52425 Jülich, Germany
[2]RWTH Aachen University, 52062 Aachen, Germany
[3]JARA Energy, 52425 Jülich, Germany

Corresponding author: Yifei Lu (yifei.lu@fz-juelich.de)

This work was supported by the Helmholtz Association under the program "Energy System Design" (ESD) and the project "Helmholtz platform for the design of robust energy systems and raw material supply (RESUR)."

ABSTRACT The gas sector is playing an increasingly important role in the decarbonization of energy systems. As a result, tools that enable the integrated analysis of power and gas networks are becoming increasingly essential. Hydrogen-blending is regarded as a promising bridging technology that can accelerate the adoption of hydrogen. However, it raises the complexity of the gas network simulation as it involves solving complex partial differential equation systems. This paper presents a new framework for the dynamic modeling and simulation of gas pipeline flows, capable of tracking the composition of gas mixtures. The proposed approach decouples the dynamic gas flow simulation and the composition tracking. The dynamic flow simulation is modeled using the central differencing and the IMEX integration scheme and represented as an equivalent electric circuit model. The derived model can then be solved using a power system EMT solver. On top of that, a batch-tracking algorithm is implemented to accurately track the propagation of the gas mixture composition in the gas pipeline network. Simulations of network models of different sizes demonstrate the advantages of this proposed modeling and simulation framework and show its potential applications in gas pipeline network analyses.

INDEX TERMS Composition tracking, dynamic simulation, electrical analogy, gas network simulation, hydrogen-blending.

I. INTRODUCTION

In recent decades, the increase in the share of renewable energy sources in power generation has contributed significantly to reducing carbon emissions in the electricity sector. However, the increasing reliance on renewable energy sources also poses new challenges and concerns regarding the robust operation of the electricity system. Electrical flexibility options that can be used to balance generation and supply patterns are critical to ensuring secure and uninterrupted power system operation [1]. Among the various electrical flexibility options, the coupling between the power and gas sectors is of particular interest [2]. On the one hand, this integration allows the power sector to leverage the enormous storage capacity of the gas sector, which can be used as seasonal storage for renewable power generation. On the other hand, comprehensive decarbonization of all energy sectors highlights the need for integrated energy systems, and this coupling contributes to the decarbonization of the gas sector by promoting the share of renewable gases. A core process in coupling the power and gas sector is the power-to-gas (PtG) process, in which electricity generated from renewable sources is converted into hydrogen or other combustible gases [3]. The produced gases can be further stored, transported, and utilized in various ways. Multiple possibilities exist for transporting hydrogen, such as transporting compressed or liquefied hydrogen using pipeline systems, using liquid organic hydrogen carriers (LOHC), or converting hydrogen to ammonia or methanol, and so on [4]. Because pure hydrogen transportation

The associate editor coordinating the review of this manuscript and approving it for publication was Chaitanya U. Kshirsagar.

technologies require new infrastructure investment, an alternative approach that has drawn considerable attention in recent years is injecting hydrogen produced using PtG technologies into the existing natural gas grid. This approach has the potential to reduce carbon emissions from the gas sector. The coupling of the electricity and gas sectors could also significantly reduce the need for grid infrastructure expansion, which is proving very difficult to implement in Germany. For example, one of the major obstacles to Germany's energy transition is that the electricity generated by wind farms in the north and east of the country cannot be fully transported to load sinks in the west and south of the country due to bottlenecks in the transmission grid. By strategically locating large electrolyzers in front of these bottlenecks, this electricity could be used locally, eliminating grid congestion. The hydrogen produced in this way could then be distributed widely using gas infrastructures [5]. However, an increasing concentration of hydrogen in the gas network poses new challenges for the gas network operation. For example, a higher hydrogen concentration reduces the energy content per unit volume of the gas mixture, leading to increased pressure drops in the gas network [6], [7], [8]. In addition, most of the current natural gas infrastructure is unsuitable for transporting gases with a high proportion of hydrogen. In most countries, the permissible hydrogen concentration in the natural gas network is below 10% [9], and the compatibility with hydrogen content in the gas mixture varies among network components [10]. At the same time, the current gas network infrastructure lacks sufficient gas measurement devices. As a result, new methods and tools are needed to accurately model and simulate gas networks with hydrogen injections in order to make reliable planning and operating decisions for the future gas grid.

This paper proposes a new modeling and simulation approach for the dynamic simulation of gas networks. The advantages and potential applications of the proposed modeling and simulation framework are shown together with the case studies. The key contributions of this work are as follows:

- A novel modeling approach using an electrical analogy that is based on the central differencing and the implicit-explicit integration scheme. The new approach is symmetric in its topology and has promising numerical performance.
- A gas composition tracking algorithm is added to the proposed modeling and simulation framework, which enables the tool to simulate gas networks with arbitrary gas mixture compositions.
- The proposed method is tested on different network cases to showcase its advantages and scalability.

II. STATE OF THE ART

The dynamic gas network simulation is usually formulated on the basis of the one-dimensional isothermal Euler equations and solved using techniques for solving partial differential equations (PDE). Although the pipeline gas flow simulation is a one-dimensional problem, its complexity increases exponentially with the size of the simulated network. Therefore, numerous research works have been conducted to investigate the possibility of improving the simulation efficiency of the dynamic gas grid simulation problem from different perspectives. In [11], the authors propose a hierarchical modeling framework to switch between the PDE system and simplified semi-linear and algebraic models to reduce the simulation time. This method enables switching between different models with different accuracy levels, which accelerates the simulation run. In addition to the effort to accelerate the simulation from the software perspective, some other research groups try to use hardware acceleration. For example, in [12], the authors implement a parallelization method with which pipelines in a network are decoupled and simulated independently. The network can then be simulated using GPUs to achieve hardware acceleration. Instead of improving the simulation speed using algorithmic or hardware accelerations, several works try to solve the computational problem by modeling the gas pipeline as equivalent electric circuits. In [13], [14], the authors present a modeling framework for the dynamic simulation of gas pipelines based on an electrical analogy, with which a pipeline model can be represented as a combination of a resistance, a voltage source, and a capacitance. However, the value of the equivalent capacity is defined as the storage capacity of the pipeline segment per unit pressure difference, which is not a rigorous mathematical derivation from the governing equations and hence cannot guarantee high simulation accuracy. To solve this issue, in [15], the authors introduce a correction factor to improve the simulation accuracy of the modeling framework mentioned previously by calibrating the simulation results with actual measurement values. However, their work does not present a universal approach to determining the correction factor, which means a fully automatic process to create an accurate electrical analogy is still impossible. In [16], the authors present a modeling and simulation framework for the dynamic simulation of gas networks. The PDEs are transformed to be represented with fundamental electrical circuit elements and solved using the resistive companion and MNA approach. The pipeline system can, therefore, be modeled and simulated using power system analysis software or tools. In [16], the simulation is solved in the power system simulation software PSCAD, and the results show great compromises in terms of simulation speed and accuracy of simulation results. However, since the modeling approach is tested only using proprietary software designed initially for power systems, its scalability in modeling and simulation has not been proven. All studies mentioned above address and contribute to the acceleration of the gas network dynamic simulation with different methods. However, tracking the composition and properties of the gas mixture during the simulation goes beyond the scope of the studies mentioned above.

Hydrogen blending into the natural gas network has attracted a lot of attention in recent years. Numerous studies have been conducted to analyze the potential and challenges of hydrogen blending into the natural gas network [7], [17], [18], [19]. However, most of these studies are based on steady-state simulations and, therefore, cannot accurately represent the actual short-term operating conditions of the natural gas network, especially when simulating gas transmission networks with hydrogen injections [20], [21], [22]. A recent study [23] focuses on tracking hydrogen concentration propagation in the dynamic simulation of transmission gas pipelines. The results show that the propagation speed of hydrogen concentration is much slower than the dynamic response of flow rate and pressure in long-distance transmission pipelines. Therefore, it is essential to model the propagation of gas mixture composition in the dynamic gas network simulation in order to obtain reliable results for analyses of hydrogen-enriched gas networks. In [24], the authors proposed a simulation framework to address the problem of tracking gas mixture composition propagation in gas network transients by adding an additional PDE. The problem PDE system is then solved using finite differences and an iterative method using the Newton-Raphson algorithm. With the additional PDE and the iterative method chosen to solve the system, the computational cost is relatively high. In [25], the authors implement two approaches to modeling the propagation of the gas mixture and tracking its composition in dynamic gas pipeline simulations. These two modeling methods are used to model a long-distance gas transmission pipeline, and the simulation results of both methods are compared with real measurements. The first method employs a mathematical formulation of the gas mixture properties calculated from gas mixture states similar to the method implemented in [24], which is directly involved in the solving process of the PDEs. In contrast, the second one is a so-called batch tracking method that tracks the propagation of the gas mixture based on the simulation time step and the gas velocity calculated at each step. Although the latter seems to be a more straightforward method, it sometimes produces even better results than the method that uses the equation of state (EOS) to calculate the gas mixture properties in the PDE system [25]. In [22], the authors extend the simulation framework proposed in [16] with the functionality of the gas mixture composition tracking. This is achieved by modeling complex gas mixture properties and tracking the propagation of gas mixture composition using the batch tracking method described in [23]. The simulation results show that distributed parameter models are necessary for accurately modeling the effects of hydrogen propagation on the gas dynamic simulation. The simulation accuracy increases with the increase in spatial discretization resolution, which in turn causes the matrix inversion operation to be performed more frequently. However, the proposed modeling and simulation framework is only tested on a minimal network with three nodes and two pipelines. Thus, its scalability cannot be validated.

It is worth noting that the dynamic simulation of gas networks has been widely studied. However, the previous studies still have notable limitations, such as:

- Most dynamic gas network simulation studies do not consider the gas mixture property changes with various gas compositions in the network.
- The studies work on hydrogen-blending are usually performed only based on steady-state simulations.
- Most of the work on dynamic simulation of hydrogen-enriched natural gas networks is only performed on prototype networks, so their scalability cannot be validated.

III. MATHEMATICAL FORMULATION OF THE DYNAMIC PIPELINE SIMULATION USING ELECTRICAL ANALOGY

The dynamic gas pipeline flow problem is usually formulated using the one-dimensional isothermal Euler equation set [26], which consists of two equations, representing the mass conservation and momentum conservation correspondingly:

$$\frac{\partial \rho}{\partial t} + \frac{\partial (\rho v)}{\partial x} = 0 \quad (1)$$

$$\frac{\partial (\rho v)}{\partial t} + \frac{\partial (\rho v^2)}{\partial x} + \frac{\partial p}{\partial x} + \rho g \sin\theta + f \frac{\rho v |v|}{2D} = 0 \quad (2)$$

where ρ is the gas mixture density, v is the gas flow velocity, p is the pressure, f is the friction factor, D is the inner diameter of the pipeline, g is the standard gravity, θ is the tilt angle of the pipeline.

In addition to the governing equations for the flow transients, in order to analyze a natural gas network with hydrogen blending, an additional differential equation to calculate propagation of the gas mixture composition c:

$$\frac{\partial c}{\partial t} + v \frac{\partial c}{\partial x} + D_x \frac{\partial^2 c}{\partial x^2} = 0 \quad (3)$$

where c is the composition of the gas mixture, v is the gas flow velocity, and D_x is the hydrogen diffusion coefficient, which can usually be neglected. As the gas density ρ is also dependent on the composition c, for a hydrogen-blended natural gas network simulation, all three PDEs above should be solved simultaneously as in [24]. Although this approach guarantees a high accuracy by comprehensively modeling the gas mixture properties, the simulation time scales up quickly with the increase in the simulated network size, as the gas mixture properties will be updated frequently. In this work, the gas composition tracking (3) is decoupled from the flow dynamics equations (1) and (2). The frequency of the gas mixture calculation is determined by the length of pipeline segments, which can be predefined ahead of the simulation and therefore offers the option to compromise between simulation speed and accuracy.

A. EQUIVALENT ELECTRIC CIRCUIT MODEL BASED ON THE UPWIND DIFFERENCING AND EXTRAPOLATION

The gas mixture density ρ is usually difficult to measure directly in real gas network operation, as it depends on the

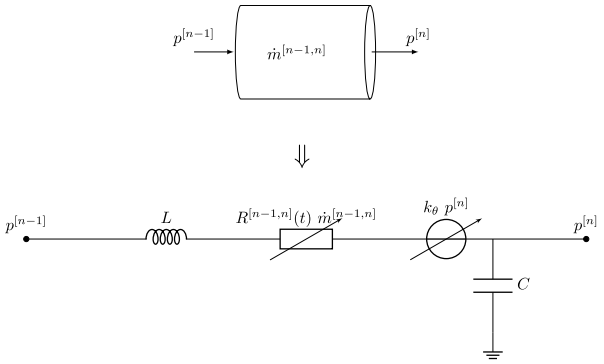

FIGURE 1. Electrical analogy model proposed in [16].

temperature, pressure, and composition of the gas mixture. Therefore, we replace it with the pressure p based on the real gas law with the compressibility factor Z(cf. [27]).

$$\rho = \frac{Mp}{ZRT} \tag{4}$$

where M is the molar mass of the gas mixture, p is the pressure, Z is the gas mixture compressibility factor, R is the universal gas constant and T is the temperature. And the flow velocity v is replaced with mass flow rate $\dot{m}$ using the definition of $\dot{m}$:

$$\rho v = \frac{\dot{m}}{A} \tag{5}$$

Neglecting the convection term $\partial(\rho v^2)/\partial x$, the above equation set can be transformed into (cf. [16]):

$$AM\frac{\partial p}{\partial t} + ZRT\frac{\partial \dot{m}}{\partial x} = 0 \tag{6}$$

$$\frac{1}{A}\frac{\partial \dot{m}}{\partial t} + \frac{\partial p}{\partial x} + \frac{pMg\sin\theta}{ZRT} + \frac{ZRT}{Mp}\frac{f\dot{m}|\dot{m}|}{2A^2D} = 0 \tag{7}$$

where A is the inner cross-sectional area of the pipeline.

In our previous work [22], the model proposed by [16] is adopted as shown in Fig. 1. The (6) and (7) are converted into an electric circuit analogy by discretizing a pipeline into multiple uniform sections:

$$C\frac{\mathrm{d}p^{[n]}}{\mathrm{d}t} = \dot{m}^{[n,n+1]} - \dot{m}^{[n-1,n]} \tag{8}$$

$$L\frac{\mathrm{d}\dot{m}^{[n-1,n]}}{\mathrm{d}t} = (p^{[n]} - p^{[n-1]}) - k_\theta p^{[n]} - R^{[n-1,n]}(t)\dot{m}^{[n-1,n]} \tag{9}$$

where

$$L = \frac{\Delta x}{A}$$

$$C = \frac{\Delta x AM}{ZRT}$$

$$R^{[n-1,n]}(t) = \frac{\Delta x f}{2AD}\frac{ZRT|\dot{m}^{[n-1,n]}|}{MAp^{[n]}}$$

$$k_\theta = \frac{\Delta x Mg\sin\theta}{ZRT}$$

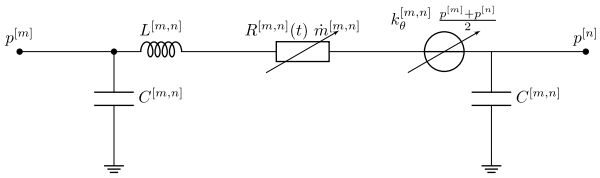

FIGURE 2. Equivalent π-model for a pipeline section (note that new indexing is used to denote the pressure at both ends of the pipe).

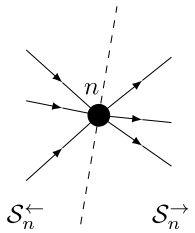

FIGURE 3. Direction of pipelines connected to a node *n*.

As the model is similar to the Γ-model for transmission lines in power systems, it is referred to as the Γ-model in the rest of the paper.

One major problem we have identified during our work is that simulations with the Γ-model depend heavily on the pipeline orientation. Specifically, due to the differencing scheme applied in the Γ-model, it results in an unsymmetrical equivalent electrical model as shown in Fig. 1. Moreover, the integration in the Γ-model presumes a positive flow direction, which means the flow direction should always match the assigned pipeline direction. One straightforward solution to this problem is to initialize the dynamic simulation with a steady-state simulation. In this way, the directions of the flows can be accurately determined and used to assign the pipeline directions. However, this method encounters practical limitations in simulating real network operations, as some pipelines can be operated in both directions. To ensure a robust solution in such cases, steady-state simulations need to be carried out frequently to ensure the flow directions are known and correctly assigned in advance so that the convergence of the following dynamic simulation can be ensured. However, this solution leads to a considerable slowdown in the dynamic simulation, which makes it unscaleable for large and complex networks.

B. EQUIVALENT ELECTRIC CIRCUIT MODEL BASED ON THE IMEX INTEGRATION SCHEME

To overcome the challenges mentioned above, a novel modeling approach is developed. The new method aims to obtain a symmetric representation (see Fig. 2) of the pipeline, so that it can ensure that the flow direction does not have a negative impact on the convergence and accuracy of the simulation.

To achieve this, we first apply a spatial discretization of (6) and generalize it at node n with multiple inflows $\mathcal{S}_n^{\leftarrow}$ and

outflows $\mathcal{S}_n^{\rightarrow}$ (see Fig. 3) and it can be transformed into:

$$\left(\sum_{i\in\mathcal{S}_n^{\rightarrow},\mathcal{S}_n^{\leftarrow}} \frac{A^i M\,\Delta x^i/2}{ZRT}\right)\frac{\mathrm{d}p^{[n]}}{\mathrm{d}t} + \left(\sum_{[n,m]\in\mathcal{S}_n^{\rightarrow}} \dot{m}^{[n,m]} - \sum_{[m,n]\in\mathcal{S}_n^{\leftarrow}} \dot{m}^{[m,n]}\right) = 0 \tag{10}$$

Applying trapezoidal rule to (10), we obtain:

$$\left(\sum_{i\in\mathcal{S}_n^{\leftarrow},\mathcal{S}_n^{\rightarrow}} \frac{A^i M\,\Delta x^i/2}{ZRT}\right)\frac{p^{[n]}(t)-p^{[n]}(t-\Delta t)}{\Delta t} + \left(\sum_{[n,m]\in\mathcal{S}_n^{\rightarrow}} \frac{\dot{m}^{[n,m]}(t)+\dot{m}^{[n,m]}(t-\Delta t)}{2}\right) - \left(\sum_{[m,n]\in\mathcal{S}_n^{\leftarrow}} \frac{\dot{m}^{[m,n]}(t)+\dot{m}^{[m,n]}(t-\Delta t)}{2}\right) = 0 \tag{11}$$

In (11), the presence of a non-linear friction term in the momentum conservation equation at (7) complicates the integration process when using implicit methods. Various strategies can be employed to address this challenge. One potential solution is the use of iterative methods, such as the Newton-Raphson algorithm, as outlined in [24]. However, this approach increases the computational cost of the simulation. In [16], the authors use an extrapolation method to approximate the non-linear terms. However, as discussed in some literature, using extrapolation for nonlinear terms is a relatively unstable approach [28]. To address this issue, the Euler IMEX integration scheme is applied to the above ODE. The linear term of the function is integrated using the Euler backward method, while the non-linear term is integrated using the Euler forward method.

Suppose a pipe section $[m, n]$ with inlet and outlet nodes m and n. The discretization of the momentum conservation equation then reads:

$$\frac{\dot{m}^{[m,n]}(t)-\dot{m}^{[m,n]}(t-\Delta t)}{\Delta t} + \underbrace{A_i\frac{p^{[n]}(t)-p^{[m]}(t)}{\Delta x^{[m,n]}} + \frac{MA^{[m,n]}g\sin\theta^{[m,n]}}{ZRT}\frac{p^{[n]}(t)+p^{[m]}(t)}{2}}_{\text{linear term implicitly discretized}} + \underbrace{\frac{f^{[m,n]}ZR}{2MA^{[m,n]}D^{[m,n]}}\frac{2\dot{m}^{[m,n]}(t-\Delta t)|\dot{m}^{[m,n]}(t-\Delta t)|}{p^{[n]}(t-\Delta t)+p^{[m]}(t-\Delta t)}}_{\text{non-linear term explicitly discretized}} = 0 \tag{12}$$

One disadvantage of this method is the first-order degree of accuracy of the Euler IMEX method. This may compromise the temporal accuracy of the momentum equation compared to the second-order accurate trapezoidal rule used in the Γ-model. This issue can be however easily addressed by applying higher-order IMEX schemes.

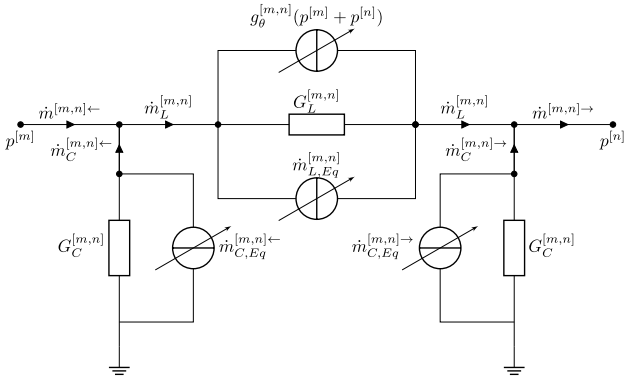

FIGURE 4. Resistive companion π-model for a pipeline section.

To implement the derived model in (11) in an MNA solver, it needs to be reformulated into a resistive companion. First, we defined dummy mass flows $\dot{m}^{i\leftarrow}$ and $\dot{m}^{i\rightarrow}$ for the inflow and outflow of the pipeline section. The sum of the incoming and outgoing dummy mass flow rates of pipelines connected to node n is zero, which means for node n, the following constraint applies:

$$\sum_{[m,n]\in\mathcal{S}_n^{\leftarrow}} \dot{m}^{[m,n]\rightarrow} - \sum_{[n,m]\in\mathcal{S}_n^{\rightarrow}} \dot{m}^{[n,m]\leftarrow} = 0 \tag{13}$$

Therefore, the capacitance and inductance mass flow rates at each pipeline section are defined as:

$$\begin{aligned}\dot{m}_C^{[m,n]\leftarrow}(t) &= \dot{m}^{[m,n]}(t) - \dot{m}^{[m,n]\leftarrow}(t)\\ &= -G_C^{[m,n]}p^{[m]}(t) + \dot{m}_{C,Eq}^{[m,n]\leftarrow}(t) \qquad (14)\\ \dot{m}_C^{[m,n]\rightarrow}(t) &= \dot{m}^{[m,n]\rightarrow}(t) - \dot{m}^{[m,n]}(t)\\ &= -G_C^{[m,n]}p^{[n]}(t) + \dot{m}_{C,Eq}^{[m,n]\rightarrow}(t) \qquad (15)\\ \dot{m}_L^{[m,n]}(t) &= \dot{m}^{[m,n]}(t)\\ &= G_L^{[m,n]}\left(p^{[n]}(t)-p^{[m]}(t)\right)\\ &\quad + g_\theta^{[m,n]}\left(p^{[n]}(t)+p^{[m]}(t)\right) + \dot{m}_{L,Eq}^{[m,n]}(t) \qquad (16)\end{aligned}$$

where the coefficients of the admittance matrix are:

$$G_L^{[m,n]} = \frac{A^{[m,n]}\Delta t}{\Delta x^{[m,n]}} \tag{17}$$

$$G_C^{[m,n]} = \frac{MA^{[m,n]}\Delta x^{[m,n]}}{ZRT\,\Delta t} \tag{18}$$

$$g_\theta^{[m,n]} = \frac{MA^{[m,n]}g\sin\theta^{[m,n]}\Delta t}{2ZRT} \tag{19}$$

and the current injection of the equivalent pipeline section:

$$\dot{m}_{C,Eq}^{[m,n]\leftarrow}(t) = G_C^{[m,n]}p_m(t-\Delta t) - \dot{m}_C^{[m,n]\leftarrow}(t-\Delta t) \tag{20}$$

$$\dot{m}_{C,Eq}^{[m,n]\rightarrow}(t) = G_C^{[m,n]}p_n(t-\Delta t) - \dot{m}_C^{[m,n]\rightarrow}(t-\Delta t) \tag{21}$$

$$\dot{m}_{L,Eq}^{[m,n]}(t) = -\Delta\dot{m}^{[m,n]}(t-\Delta t) + \dot{m}_L^{[m,n]}(t-\Delta t) \tag{22}$$

The nonlinear friction term is contained in the term $\Delta\dot{m}^{[m,n]}$ expressed as:

$$\Delta\dot{m}^{[m,n]}(t-\Delta t) = \frac{f^{[m,n]}ZRT\,\Delta t}{MA^{[m,n]}D^{[m,n]}} \cdot \frac{\dot{m}^{[m,n]}(t-\Delta t)|\dot{m}^{[m,n]}(t-\Delta t)|}{p^{[n]}(t-\Delta t)+p^{[m]}(t-\Delta t)} \tag{23}$$

This formulation makes sense since summing up (14) of $\mathcal{S}_n^{\leftarrow}$ and (15) of $\mathcal{S}_n^{\rightarrow}$ recovers (11) due to (13). Meanwhile, (12) is captured by (16). Finally, subtracting (14) from (16) and adding (15) and (16) yields two equations which can be represented in matrix form:

$$\underbrace{\begin{bmatrix} G_L^{[m,n]}+G_C^{[m,n]}-g_\theta^{[m,n]} & -G_L^{[m,n]}-g_\theta^{[m,n]} \\ -G_L^{[m,n]}+g_\theta^{[m,n]} & G_L^{[m,n]}+G_C^{[m,n]}+g_\theta^{[m,n]} \end{bmatrix}}_{G^{[m,n]}} \underbrace{\begin{bmatrix} p^{[m]}(t) \\ p^{[n]}(t) \end{bmatrix}}_{x^{[m,n]}}$$
$$= \underbrace{\begin{bmatrix} \dot{m}_{C,Eq}^{[m,n]\leftarrow}(t)-\dot{m}_{L,Eq}^{[m,n]}(t)+\dot{m}^{[m,n]\leftarrow}(t) \\ \dot{m}_{C,Eq}^{[m,n]\rightarrow}(t)+\dot{m}_{L,Eq}^{[m,n]}(t)-\dot{m}_i^{[m,n]\rightarrow}(t) \end{bmatrix}}_{b^{[m,n]}} \tag{24}$$

The full matrix system $Gx = b$ can be constructed by summing the coefficients of the stamp matrix at each nodes. The dummy mass flow rates will then cancel each other due to (13). In the case of a straight pipeline where each section has the same parameters, then:

$$G = \begin{bmatrix} G_a & G_b & 0 & \cdots & \cdots & \cdots & 0 \\ G_c & G_d & G_b & 0 & & & \vdots \\ 0 & G_c & G_d & G_b & \ddots & & \vdots \\ \vdots & 0 & \ddots & \ddots & \ddots & \ddots & \vdots \\ \vdots & & \ddots & \ddots & \ddots & \ddots & 0 \\ \vdots & & & \ddots & G_c & G_d & G_b \\ 0 & \cdots & \cdots & \cdots & 0 & G_c & G_e \end{bmatrix} \tag{25}$$

$$x = \begin{bmatrix} p_1 & \dots & p_N \end{bmatrix} \tag{26}$$

$$b = \begin{bmatrix} b_1 & \dots & b_N \end{bmatrix} \tag{27}$$

with:

$$\begin{aligned} G_a &= G_L + G_C - g_\theta \\ G_b &= -G_L - g_\theta \\ G_c &= -G_L + g_\theta \\ G_d &= 2G_L + 2G_C \\ G_e &= G_L + G_C + g_\theta \end{aligned}$$

and

$$\begin{aligned} b_1 &= \dot{m}_{C,Eq}^{[1,2]\leftarrow} - \dot{m}_{L,Eq}^{[1,2]} + \dot{m}_{\text{in}} \\ b_i &= \dot{m}_{C,Eq}^{[i-1,i]\rightarrow} + \dot{m}_{L,Eq}^{[i-1,i]} + \dot{m}_{C,Eq}^{[i,i+1]\leftarrow} - \dot{m}_{L,Eq}^{[i,i+1]} \\ b_N &= \dot{m}_{C,Eq}^{[N-1,N]\rightarrow} + \dot{m}_{L,Eq}^{[N-1,N]} - \dot{m}_{\text{out}} \end{aligned}$$

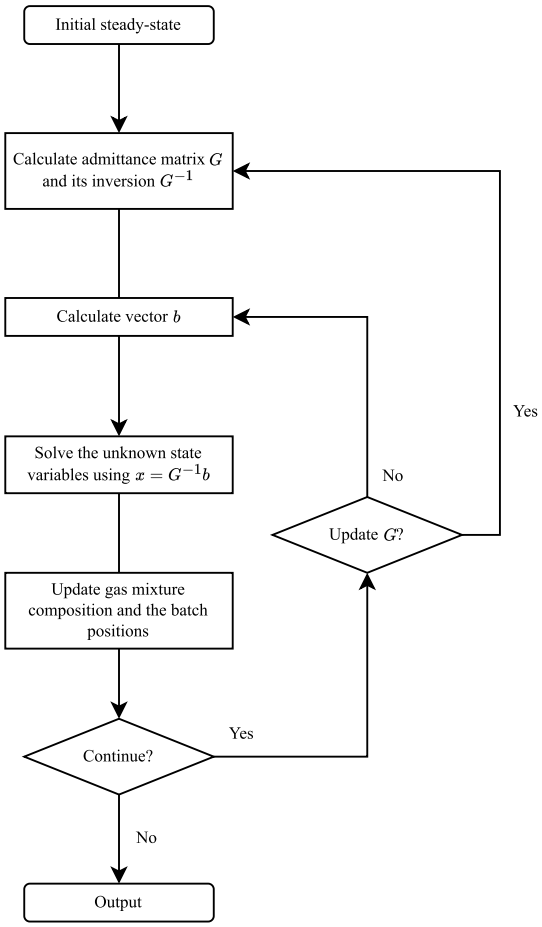

FIGURE 5. Overview of the simulation solution flow.

It can be noted that the coefficient $g_\theta^{[m,n]}$ of the voltage-controlled current source is also included in the admittance matrix calculation. Therefore, no additional memory and calculation is required to account for the effect of height differences on the pipeline flow dynamics.

C. INTEGRATION WITH THE BATCH-TRACKING ALGORITHM

The simulation solution flow overview is shown in Fig. 5. To start the dynamic simulation, the system must first reach a steady state. This can be achieved either by using a separate steady-state gas network simulation solver or by running the dynamic simulation until it reaches the steady state. Because of the different simplifications applied to the dynamic and steady-state models, there are always minor differences in the steady-state simulation results. Therefore, in this paper, all initial steady states for the simulation are achieved directly using the dynamic simulation solver. After initializing the simulation setup, the admittance matrix G and its inversion matrix G^{-1} are calculated. Because of the high computational cost of the matrix inversion calculation for large systems, both matrices will only be updated when the analog admittance G_L, G_C, or G_θ is changed. The vector b, which contains the known variables, is then updated. The vector of unknowns

x can then be calculated with $x = G^{-1}b$. After calculating the state variables, the gas mixture composition tracking algorithm is applied to update the batch head positions and, if applicable, the nodal gas mixture compositions. For the gas mixture composition tracking, the batch tracking algorithm is adopted as shown in (28) (cf. [25]).

$$z_j^{[m,n]}(t) = z_j^{[m,n]}(t - \Delta t) + v^{[m,n]}(t)\Delta t \tag{28}$$

where $z_j^{[m,n]}$ is the location of the jth batch head in the pipeline connecting nodes m and n. If the position of the batch head $z_j^{[m,n]}(t)$ is greater than the length of the corresponding pipeline, the outlet composition of this pipeline is updated with the corresponding composition $c^{[m,n]}$. The gas mixture at the junction node n can be updated using (29).

$$c^{[n]} = \frac{\sum\limits_{[m,n]\in\mathcal{S}_n^{\leftarrow}} Q^{[m,n]}c^{[m,n]} + \sum\limits_{[n,m]\in\mathcal{S}_n^{\rightarrow}} Q^{[n,m]}c^{[n,m]}}{\sum\limits_{[m,n]\in\mathcal{S}_n^{\leftarrow}} Q^{[m,n]} + \sum\limits_{[n,m]\in\mathcal{S}_n^{\rightarrow}} Q^{[n,m]}} \tag{29}$$

The above steps are repeated until the simulation ends, and the results are saved and output.

One thing to note is that the burnable gases have different heating values, which means that the actual gas mass flow rate can vary depending on the composition of the gas mixture that reaches the end consumer. Therefore, the corresponding gas flow rate should also be updated to reflect the actual gas mixture heating value after the gas batch head arrives at the demand. To simplify the simulation, we assume the considered gas mixture to be a binary mixture consisting of only methane and hydrogen, thereby reducing the number of state variables that need to be considered. At high pressures, real gas behavior deviates from the ideal gas, and the compressibility factor Z is typically determined using EOS models. However, involving complex EOS models in the dynamic simulation can be computationally expensive. An easy workaround is to apply linear mixing models for the compressibility factor calculation, as shown in [18], which can slightly improve accuracy without significantly increasing computational costs. In this work, we adopt the ideal gas law by assuming a constant compressibility factor $Z = 1$ for simplicity. The molar mass M and the HHV of the gas mixtures are calculated using linear mixing rules.

IV. SIMULATION STUDY CASES AND DISCUSSION

For the simulations, the Π-model derived in the previous section is implemented in an MNA-based power system EMT simulation solver and used to simulate networks with different sizes. In this work, all simulations are performed on an AMD Ryzen Threadripper 3960X machine, which has 24 cores and 256 GB RAM and runs Ubuntu OS 20.04.6.

A. SIMULATION OF A SINGLE PIPELINE

First, the simulations are performed on a single pipeline with different settings. The simulation results are compared with the Γ-model to validate its accuracy and illustrate the advantages of the proposed modeling approach. The considered pipeline parameters are listed in Table 1.

TABLE 1. Pipeline parameters.

Pipeline parameters	Values
Diameter [m]	0.6
Inclination angle	0
Length [m]	50000
Section length [m]	5000
Number of sections	10

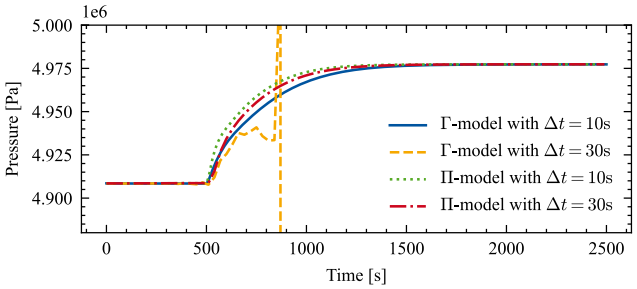

FIGURE 6. Pressure at the pipeline outlet after demand drop from 20 kg/s to 10 kg/s.

For the first simulation case, the pipeline inlet (left) is connected with a pressure source that has a constant pressure value of 50 bar. The pipeline outlet (right) is connected to a demand of 20 kg/s. In order to observe the transient gas flow dynamics, the demand at the pipeline outlet is changed from 20 kg/s to 10 kg/s at 500 s. For this simulation case, different time steps are chosen for both modeling methods. As can be seen from Fig. 6, the simulations with the method proposed in this paper converge with time steps of both 10 s and 30 s. However, the Γ-model only converges with a time step of 10 s. For a time step of 30 s, the simulation quickly diverges at around 380 s after the change in demand. Therefore, it can be concluded that the proposed Π-model generally exhibits better numerical stability than the previous model, which allows simulation with larger time steps.

As previously discussed, one major issue observed with the Γ-model is its validity for simulations involving reverse flow directions. Therefore, the positions of demand and source are swapped for the second scenario. The boundary conditions remain the same with 50 bar for the pressure and 20 kg/s for the demand. The simulation results are shown in Fig. 7. It can be observed that the simulation with the Π-model converges with time steps of 1, 10, and up to 30 s. The final state of the outlet (left) pressure remains almost the same as the initial state in the previous case. This confirms the effectiveness of the Π-model under this system setting. However, the simulation results with the Γ-model show strong oscillations, and it does not converge. With the simulation time step of 30 s, the simulation with the Γ-model diverges rapidly after the start of the simulation and the results are therefore not shown in this figure.

For the next simulation case, we apply a negative demand at the pipeline inlet (left), i.e., gas is fed into the pipeline. The value of the pressure at the outlet (right) is set based on the

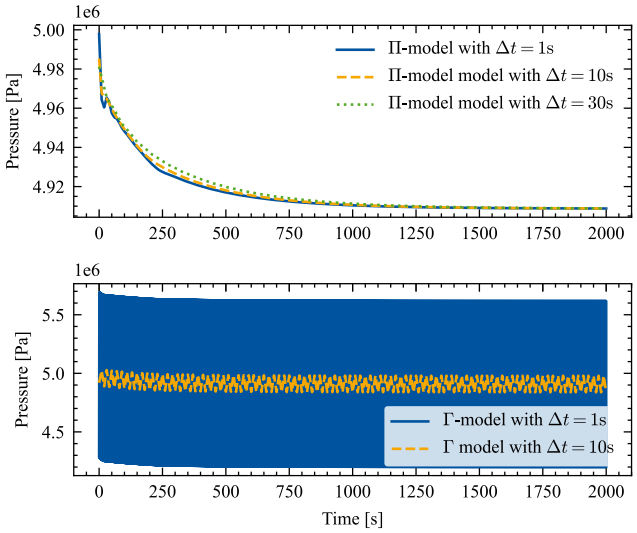

FIGURE 7. Pressure at the pipeline outlet (left) with reversed supply and demand connection.

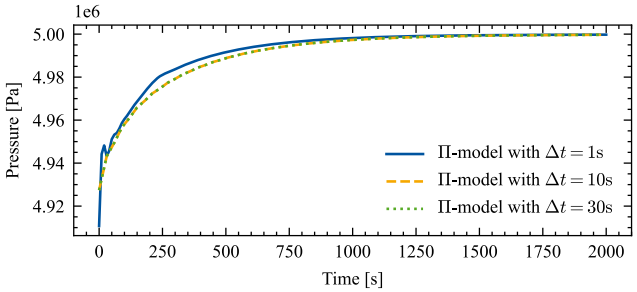

FIGURE 8. Pressure at pipeline inlet (left) with reversed flow direction.

steady-state calculated from the previous cases. Therefore, the operational situation of the pipeline should be the same as the base scenario. However, the simulations with the Γ-model do not converge even with a time step of 1 s. Therefore, only simulation results with the Π-model are shown in Fig. 8. It can be seen that the final state of the pipeline inlet (left) pressure is around 50 bar, which corresponds to the pressure value used for previous simulation cases.

For the final case, a simulation with hydrogen tracking is employed on this single pipeline model. The hydrogen concentration is set to 0 at the beginning of the simulation, and it increases to 20 vol% at 20000 s. For this simulation, different section lengths are chosen for spatial discretization, and the simulation results are shown in Fig. 9. After the change of the gas mixture composition at 20000 s, the pressure at the pipeline outlet first begins to drop due to the propagation of hydrogen in the pipeline. After the gas mixture reaches the end of the pipeline, the actual gas flow rate is updated based on the gas mixture heating value to meet the same energy demand of the end user. In this simulation case, this results in a slight increase in pressure at the pipeline outlet. It can be seen from the results that the pressure at the pipeline outlet changes in a step-wise manner with a larger section length setting. By reducing the section length, the pressure changes become smoother

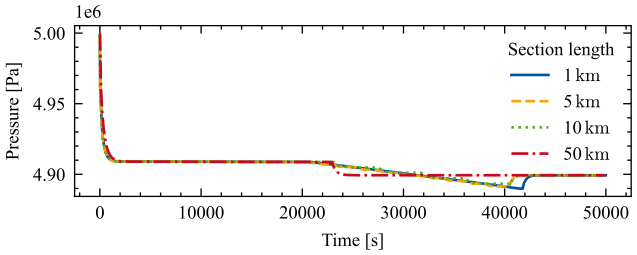

FIGURE 9. Outlet pressure considering hydrogen propagation in the gas pipeline.

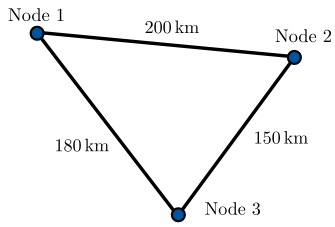

FIGURE 10. A simple 3-node network.

TABLE 2. Node parameters.

	Known states	Altitudes	Temperature
Node 1	50 bar	100 m	300 K
Node 2	20 sm^3/s	40 m	288.15 K
Node 3	50 sm^3/s	50 m	288.15 K

and even almost linear when the section length is set to be 1 km. Another finding from this result is that with a smaller section length, a lower minimal outlet pressure can be observed. This is significant because the pressure drop is an essential criterion in evaluating the safety of the gas network operation. At the same time, a reduction in the section length leads to a quadratic increase in the size of the simulation problem, which worsens even further when calculating the matrix inversion. It is therefore essential to choose a suitable spatial discretization resolution so that a compromise can be achieved between computation time and the reliability of the results.

To briefly wrap up the simulation results of a single pipeline, it can be concluded that simulations with the Π-model show a better numerical stability behavior. Because the gas dynamics are usually much slower than 1 second, a more numerically stable approach can significantly reduce the necessary simulation time by simply enlarging the simulation time step.

B. SIMULATION OF A SMALL TRIANGLE NETWORK

In this subsection, simulations are performed on a simple fictitious triangle network to further demonstrate the advantages of the proposed modeling approach. Since a triangle network is the minimal network one can imagine, it can be used as a prototype and to validate the modeling approach and the corresponding simulation framework.

The parameters of the network nodes are listed in Table 2. The pipeline lengths are marked in Fig. 10 and all three

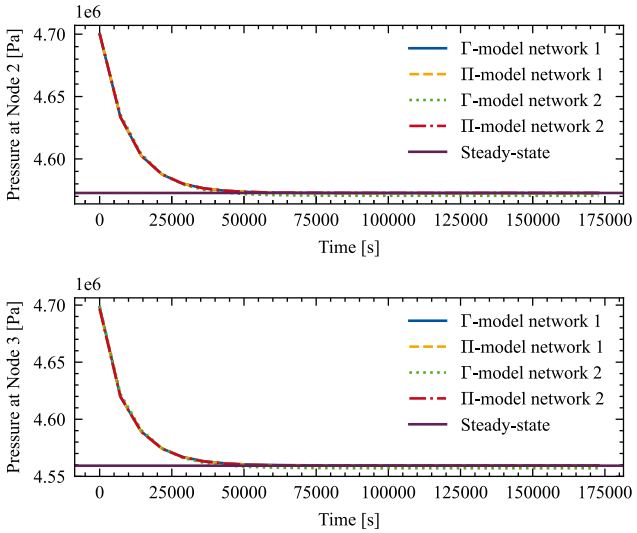

FIGURE 11. Pressure at node 2 (above) and node 3 (below).

pipelines have a diameter of 0.5 m and a friction factor of 0.01.

For this network, three different network settings are considered:

1) Pipeline direction assigned as shown in Fig. 10
2) Reversed pipeline direction of the pipeline between Node 1 and Node 3
3) Reversed pipeline direction of the pipeline between Node 1 and Node 2

An initial pressure of 47 bar is set for nodes 2 and 3 to start the simulation. The simulation time step for the Π-model is 30 s, while for simulations with the Γ-model it is set to 10 s. The simulation results with the first two network settings are shown in Fig. 11. It can be observed that both simulation results for the first network configuration are almost identical. For the second network setting, the final steady-state pressure values calculated using the Γ-model are slightly lower than the results of the simulation of the first network configuration. This finding further confirms the discussion in the previous sections that the Γ-model cannot guarantee accuracy when the pipeline flow directions are unknown due to the unsymmetrical topology.

It is to be noted that for the third system setting, the network simulation using the Γ-model no longer converges, while simulations with the Π-model still converge with a simulation time step of 10 s. In combination with the previous simulation results of a single pipeline with the reversed flow, it can be concluded that the Γ-model loses its effectiveness if there is a node in the system where none of the connected pipelines have the same flow direction as the assigned pipeline direction. In such a system setup, the gas demand, which is modeled as a current source in the analog electrical circuit, is no longer connected to a capacitor. The analogical capacity represents the damping effect in the mass conservation equation ((8)).

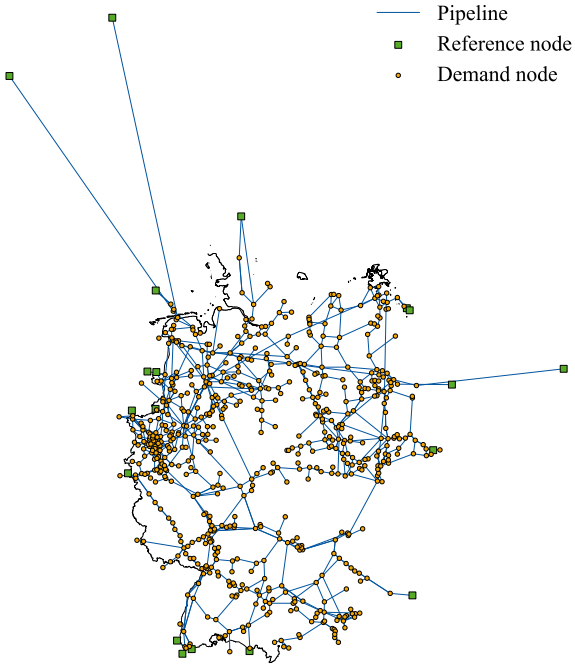

FIGURE 12. The German gas transmission network model.

C. SIMULATION OF THE GERMAN NATURAL GAS NETWORK

To test the scalability of the proposed modeling and simulation framework, it is now implemented to perform a dynamic simulation of the German gas transmission network. The gas network model is generated based on open-source datasets comprising a total of 658 nodes and 1019 pipelines.

The network topology data is based on the `SciGRID_gas` network dataset, an open-source network topology dataset based on publicly available data, including map data from `OpenStreetMap` [29], press releases, internet data, and other sources. In addition to the network topology data, the demand at the network nodes is needed to perform a gas network simulation. To achieve this, the demand disaggregation tool `DemandRegio` [30] is used to generate demand data with hourly temporal resolution and NUTS-3 spatial resolution for Germany. To balance the network demand, we assign 13 pressure reference nodes, which are mainly the import nodes where gas flows into Germany [31]. The other cross-border points are considered to be demand nodes and the corresponding flow rates are assigned with values available from the German Federal Network Agency (Bundesnetzagentur) website [32]. For more details on the network model, please refer to the following work [33].

To start the simulation, a pressure of 70 bar is assumed at all nodes in the network. Due to the uneven distribution of the pipeline length in the network, the section length is set to 20 km, which means pipelines with a length shorter than 20 km are not discretized. Because of the high complexity of the network and possible reverse flows, simulations with a time step Δt of 1 s do not converge

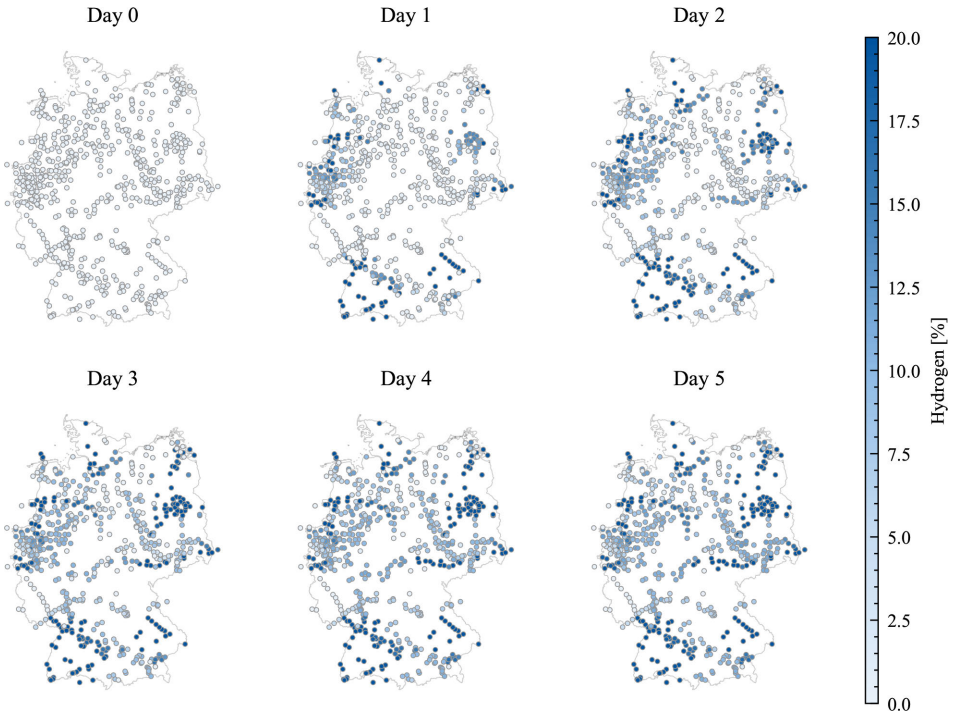

FIGURE 13. Nodal hydrogen fraction values when all import nodes have a hydrogen concentration of 20 vol%.

with the Γ-model. In contrast, the network simulation using the Π-model converges within 40 seconds for a daily simulation with a simulation time step Δt of 1 s. However, the simulation no longer converges after increasing the simulation time step. One possible explanation is the highly uneven distribution of the pipeline length in the network (see Fig. 14), which in turn results in a poorly conditioned admittance matrix. A comparison of simulation times using different methods is shown in Table 3. In this comparison, the proposed electrical analogy (EA) approach is evaluated against a non-optimized finite difference (FD) formulation, as described in equations (6) and (7). For both methods, the composition tracking (CT) algorithm is applied and compared with cases where the gas mixture in the network is assumed to have a single composition (SC). All simulations are performed on the German network model over 24 hours to ensure a representative number of composition tracking and mixing operations for both CT cases. It can be observed that for single-composition simulations, the proposed EA method significantly outperforms the FD approach. This speedup is attributed to the EA method being solved via the MNA solver, which requires only a single matrix inversion at the start of the simulation. In contrast, the FD approach requires a matrix inversion at every time step, which has an $\mathcal{O}(n^3)$ complexity. When comparing FD+CT with FD+SC, a small overhead from the composition tracking algorithm can be noticed, averaging around 6 ms per simulation step. This indicates the decoupled batch tracking algorithm does not result in a significant slowdown of the overall performance. However, the total simulation time of EA+CT is noticeably higher than expected, which is the sum of matrix inversion and composition tracking time. A likely explanation is the overhead caused by managing and handling cached batch composition and location information. For the FC+CT case, these data are cleared at every step immediately after the matrix inversion is performed. In contrast, for the EA+CT case, the matrix inversion is performed only when a batch reaches the end of a pipeline section. Therefore, the size of vectors used to save the batch location and composition states increases, leading to higher memory access overhead.

TABLE 3. Performance comparison with and without composition tracking (CT) using the proposed electrical analogy (EA) and finite difference (FD) methods.

	EA+CT	FD+CT	EA+SC	FD+SC
Total solving time [s]	2209	24380	36990	23829
Solving time per step [ms]	25.6	282	0.0428	276
Number of matrix inversions	2896	86400	1	86400

Here, we also conduct a hydrogen tracking simulation on the German gas grid model. To date, although many countries and network operators have set guidelines on the hydrogen blending ratio limit, there is no general limit for the maximum permissible hydrogen concentration in the gas network. In Germany, the current regulatory recommendation is 10 vol%, while the regulatory association is currently also investigating a higher blending ratio up to 20 vol%. Therefore, a 20% hydrogen blending ratio is considered for the following composition tracking scenarios. For the first

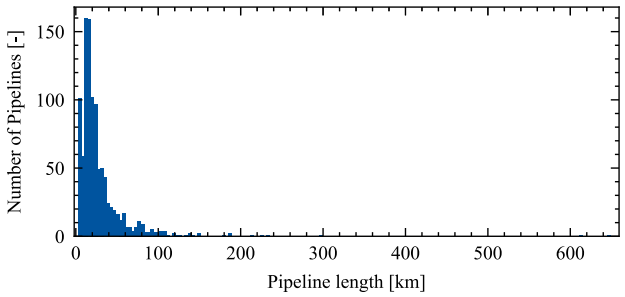

FIGURE 14. Histogram of the pipeline lengths in the German gas transmission network model.

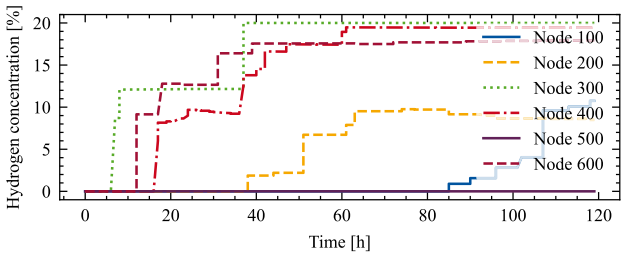

FIGURE 15. Nodal hydrogen concentration changes during the simulation run.

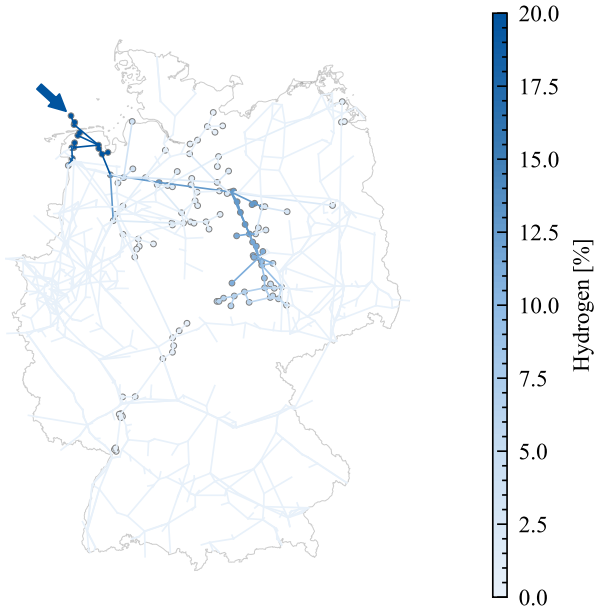

FIGURE 16. Nodal hydrogen concentration with 20 vol% hydrogen blending ratio from Norway.

case study, it is assumed that there is no hydrogen content at the beginning of the simulation, and the entire network is filled with 100% methane. Then, we increase the hydrogen concentration at all reference nodes from 0 to 20 vol%. The corresponding simulation results are shown in Fig. 13.

It can be observed that at the beginning of the simulation (day 0), there is no hydrogen in the network, and it gradually spreads from the reference nodes into the network over time. The figure also shows that the propagation rate is relatively higher at the beginning and becomes slower over the later days. This can be explained by the fact that the gas flow rates in the pipelines near the import nodes are usually higher than those near the end consumers. For a more detailed examination of the changes in the nodal hydrogen concentrations, several nodes are selected based on their indices to show how the nodal hydrogen concentration changes. The results can be found in Fig. 15.

This case study proves the scalability of the presented approach. Furthermore, it also highlights the importance of modeling the hydrogen propagation process in the gas network simulations. In Fig. 13, it is evident that even after five days of network operation, the hydrogen concentration at the network nodes is still not at 20 vol% everywhere. However, if a steady-state simulation is chosen to perform the simulation, the hydrogen concentration would immediately be updated to 20 vol% at each node. In grid operation, strong fluctuations in the hydrogen injection rate can potentially lead to significant uncertainties in the simulation results.

The assumption in the previous study is somewhat unrealistic because gas compositions from different origins typically vary in real-world network operations. Therefore, in the following case study, a single nodal hydrogen injection with 20 vol% from Norway is considered. The composition of all other import nodes is considered to be pure methane, and the simulation is run until the nodal gas composition values reach the steady state. The simulation result is shown in Fig. 16. This figure shows that the highest hydrogen concentration is in northwestern Germany, where the connections from Norway land. The gas flow is then further transported toward the southeast, with a slight margin to the south. This is interesting in light of the recent changes in the current gas supply situation in Germany. Since the Russian gas supply cutoff to Germany, more parts of Germany have been supplied with Norwegian gas. Therefore, with the gas composition tracking algorithm, a better estimation of the gas properties can be derived. If hydrogen blending is widely adopted in the future, using the gas composition tracking algorithm together with gas dynamic simulation can be crucial in making reliable grid planning and operational decisions.

V. CONCLUSION AND OUTLOOK

In this paper, a novel electrical analogy modeling framework for gas pipeline networks is presented. The proposed modeling approach is based on the central differencing scheme and uses the Euler IMEX method for time-stepping. The IMEX integration scheme enhances numerical stability by integrating the nonlinear term in the differential equation using an explicit integration method instead of using extrapolation or simply fixing the term. In addition, the chosen discretization scheme results in a symmetric equivalent circuit model, which enables improved performance when simulating networks with reverse flows, especially when simulating large-scale networks where the pipeline flow directions are usually unknown prior to the simulation. Furthermore, the method includes an algorithm for tracking the composition of the gas mixture based on the batch-tracking approach. Several

simulations are performed to compare the proposed modeling approach with the simulation results of a previously deployed model based on the Γ-model. The proposed modeling and simulation framework is also tested on a large-scale network using the German gas grid as an example, which shows the promising scalability of the approach presented in this paper.

As mentioned previously in the paper, the applied Euler IMEX integration scheme is a first-order method, which does not offer as high accuracy as other higher-order methods. To address this issue, higher-order integration methods can be implemented to achieve higher accuracy. At the same time, the proposed IMEX network is easily parallelizable, enabling further acceleration of the simulation runtime.

REFERENCES

[1] J. Adams, M. O'Malley, and K. Hanson, *Flexibility Requirements and Potential Metrics for Variable Generation: Implications for System Planning Studies*. Princeton, NJ, USA: NERC, 2010.

[2] L. Van Nuffel, J. G. Dedecca, T. Smit, and K. Rademaekers, "Sector coupling: How can it be enhanced in the Eu to foster grid stability and decarbonise?" European Parliament, Brussels, Belgium, Tech. Rep. PE 626.091, 2018. [Online]. Available: https://www.elia.be/-/media/project/elia/elia-site/public-consultations/2021/20211105_trinomics-eu-parliament-sector-coupling.pdf

[3] M. Thema, F. Bauer, and M. Sterner, "Power-to-gas: Electrolysis and methanation status review," *Renew. Sustain. Energy Rev.*, vol. 112, pp. 775–787, Jun. 2019.

[4] R. O. Cebolla, F. Dolci, and E. R. Weidner, "Assessment of hydrogen delivery options," Joint Res. Centre (JRC), Luxembourg, Tech. Rep. JRC130442, 2022. [Online]. Available: https://publications.jrc.ec.europa.eu/repository/handle/JRC130442

[5] K. Görner and D. Lindenberger, Eds., *Virtuelles Institut Strom zu Gas und Wärme-Flexibilisierungsoptionen IM Strom-Gas-Wärme-System*, vol. 1. Gütersloh, Germany: Abschlussbericht, 2018.

[6] M. Deymi-Dashtebayaz, A. Ebrahimi-Moghadam, S. I. Pishbin, and M. Pourramezan, "Investigating the effect of hydrogen injection on natural gas thermo-physical properties with various compositions," *Energy*, vol. 167, pp. 235–245, Jan. 2019.

[7] Y. Lu, T. Pesch, and A. Benigni, "Simulation of coupled power and gas systems with hydrogen-enriched natural gas," *Energies*, vol. 14, no. 22, p. 7680, Nov. 2021.

[8] I. Silvestre, R. Pastor, and R. C. Neto, "Power losses in natural gas and hydrogen transmission in the Portuguese high-pressure network," *Energy*, vol. 272, Jun. 2023, Art. no. 127136.

[9] IEA. (2018). *Limits on Hydrogen Blending in Natural Gas Networks*. Paris. [Online]. Available: https://www.iea.org/data-and-statistics/charts/limits-on-hydrogen-blending-in-natural-gas-networks-2018

[10] J. Bard, N. Gerhardt, P. Selzam, M. Beil, M. Wiemer, and M. Buddensiek, "The Limitations of Hydrogen Blending in the European Gas Grid: A study on the use, limitations and cost of hydrogen blending in the European gas grid at the transport and distribution level," Fraunhofer IEE, Berlin, Germany, Tech. Rep., Jan. 2022.

[11] P. Bales, O. Kolb, and J. Lang, "Hierarchical modelling and model adaptivity for gas flow on networks," in *Computational Science—ICCS 2009* (Lecture Notes in Computer Science), vol. 5544. Cham, Switzerland: Springer, 2009, pp. 337–346.

[12] Y. Xiang, P. Wang, B. Yu, and D. Sun, "GPU-accelerated hydraulic simulations of large-scale natural gas pipeline networks based on a two-level parallel process," *Oil Gas Sci. Technol. Revue d'IFP Energies Nouvelles*, vol. 75, p. 86, 2020, doi: 10.2516/ogst/2020076.

[13] W. Tao and H. C. Ti, "Transient analysis of gas pipeline network," *Chem. Eng. J.*, vol. 69, no. 1, pp. 47–52, Feb. 1998.

[14] S. Ke, "Transient analysis of isothermal gas flow in pipeline network," *Chem. Eng. J.*, vol. 76, no. 2, pp. 169–177, Feb. 2000.

[15] M. Taherinejad, S. M. Hosseinalipour, and R. Madoliat, "Dynamic simulation of gas pipeline networks with electrical analogy," *J. Brazilian Soc. Mech. Sci. Eng.*, vol. 39, no. 11, pp. 4431–4441, Nov. 2017.

[16] R. Song, Y. Xia, Y. Chen, S. Du, K. Strunz, Y. Song, and W. Fang, "Efficient modelling of natural gas pipeline on electromagnetic transient simulation programs," *IET Renew. Power Gener.*, vol. 17, no. 1, pp. 186–198, Jan. 2023.

[17] S. Pellegrino, A. Lanzini, and P. Leone, "Greening the gas network—The need for modelling the distributed injection of alternative fuels," *Renew. Sustain. Energy Rev.*, vol. 70, pp. 266–286, Apr. 2017.

[18] Y. Lu, T. Pesch, and A. Benigni, "GasNetSim: An open-source package for gas network simulation with complex gas mixture compositions," in *Proc. Open Source Model. Simul. Energy Syst. (OSMSES)*, Apr. 2022, pp. 1–6.

[19] D. Zhou, S. Yan, D. Huang, T. Shao, W. Xiao, J. Hao, C. Wang, and T. Yu, "Modeling and simulation of the hydrogen blended gas-electricity integrated energy system and influence analysis of hydrogen blending modes," *Energy*, vol. 239, Jan. 2022, Art. no. 121629.

[20] K. Liu, L. T. Biegler, B. Zhang, and Q. Chen, "Dynamic optimization of natural gas pipeline networks with demand and composition uncertainty," *Chem. Eng. Sci.*, vol. 215, Dec. 2019, Art. no. 115449.

[21] S. Mhanna, I. Saedi, P. Mancarella, and Z. Zhang, "Coordinated operation of electricity and gas-hydrogen systems with transient gas flow and hydrogen concentration tracking," *Electr. Power Syst. Res.*, vol. 211, Oct. 2022, Art. no. 108499.

[22] Y. Lu, T. Pesch, and A. Benigni, "Hydrogen concentration tracking in a dynamic hydrogen-enriched natural gas system based on electrical analogy," in *Proc. Int. Conf. Clean Electr. Power (ICCEP)*, Jun. 2023, pp. 746–751.

[23] D. Zhou, C. Wang, S. Yan, Y. Yan, Y. Guo, T. Shao, T. Li, X. Jia, and J. Hao, "Dynamic modeling and characteristic analysis of natural gas network with hydrogen injections," *Int. J. Hydrogen Energy*, vol. 47, no. 78, pp. 33209–33223, Sep. 2022.

[24] Z. Zhang, I. Saedi, S. Mhanna, K. Wu, and P. Mancarella, "Modelling of gas network transient flows with multiple hydrogen injections and gas composition tracking," *Int. J. Hydrogen Energy*, vol. 47, no. 4, pp. 2220–2233, Nov. 2021.

[25] M. Chaczykowski and P. Zarodkiewicz, "Simulation of natural gas quality distribution for pipeline systems," *Energy*, vol. 134, pp. 681–698, Jun. 2017.

[26] R. J. LeVeque, *Finite-Volume Methods for Hyperbolic Problems* (Cambridge Texts in Applied Mathematics). Cambridge, U.K.: Cambridge Univ. Press, 2002.

[27] R. D. Zucker and O. Biblarz, *Fundamentals of Gas Dynamics*. Hoboken, NJ, USA: Wiley, 2019.

[28] J. M. Varah, "Stability restrictions on second order, three level finite difference schemes for parabolic equations," *SIAM J. Numer. Anal.*, vol. 17, no. 2, pp. 300–309, Apr. 1980.

[29] OpenStreetMap Contributors. (2017). *Planet Dump*. [Online]. Available: https://planet.osm.org

[30] F. Gotzens, B. Gillessen, S. Burges, W. Hennings, J. Müller-Kirchenbauer, S. Seim, P. Verwiebe, T. Schmid, F. Jetter, and T. Limmer, *DemandRegio—Harmonisierung und Entwicklung von Verfahren zur Regionalen und Zeitlichen Auflösung von Energienachfragen–Abschlussbericht*. Berlin, Germany: Forschungszentrum Jülich GmbH, Jülich and Technische Universität, Berlin and Forschungsstelle für Energiewirtschaft, München, 2020.

[31] Bundesnetzagentur. (2024). *Gasimporte*. [Online]. Available: https://www.bundesnetzagentur.de/DE/Gasversorgung/aktuelle_gasversorgung/_svg/Gasimporte/Gasimporte.html

[32] Bundesnetzagentur. (2024). *Gasexporte*. [Online]. Available: https://www.bundesnetzagentur.de/DE/Gasversorgung/aktuelle_gasversorgung/_svg/Gasexporte/Gasexporte.html

[33] L. Di Francesco, "Modelling and simulation of the German gas transmission network with hydrogen blending," M.S. thesis, Politecnico di Torino, Turin, Italy, 2023. Accessed: Nov. 10, 2023. [Online]. Available: https://webthesis.biblio.polito.it/28419/

YIFEI LU (Graduate Student Member, IEEE) received the B.Sc. degree from China University of Mining and Technology, Xuzhou, China, 2016, and the M.Sc. degree from the University of Duisburg-Essen, Duisburg, Germany, in 2019. He is currently pursuing the Ph.D. degree in mechanical engineering with the Institute of Climate and Energy Systems, Energy Systems Engineering (ICE-1), Forschungszentrum Julich, Julich, Germany.

ANDREW IVAN SULIMRO received the B.Sc. degree from the University of Duisburg-Essen, Duisburg, Germany, in 2021, and the M.Sc. degree from the RWTH Aachen University, Aachen, Germany, in 2024. He is currently pursuing the Ph.D. degree with the Department of Tokamak Theory, Max Planck Institute for Plasma Physics, Garching, Germany.

THIEMO PESCH received the Diploma degree in management, business, and economics from the RWTH Aachen University, and the Electrical Engineering and Information Technology degrees in electrical power engineering from RWTH Aachen University in Germany and Chalmers University of Technology, Gothenburg, Sweden. He then wrote his dissertation, titled *Multiscale Modelling of Integrated Energy and Electricity Systems* with the Institute of Energy and Climate Research: Systems Analysis and Technology Evaluation, Forschungszentrum Jülich, Jülich, Germany. Since 2019, he has been with the Institute of Climate and Energy Systems, Energy Systems Engineering (ICE-1), Forschungszentrum Jülich, where he has led the Energy Grids department, since 2020. Since 2022, he has been with the Department of High Performance Computing.

ANDREA BENIGNI (Senior Member, IEEE) received the B.Sc. and M.Sc. degrees from Politecnico di Milano, Milano, Italy, in 2005 and 2008, respectively, and the Ph.D. degree from RWTH-Aachen University, Aachen, Germany, in 2013.

From 2014 to 2019, he was an Assistant Professor with the Department of Electrical Engineering, University of South Carolina, Columbia, SC, USA. Since 2019, he has been a Full Professor with the RWTH-Aachen and the Director of the Institute of Energy Climate Research, Energy Systems Engineering (ICE-1), Forschungszentrum Jülich.